Research Square

Preprints are preliminary reports that have not undergone peer review.
They should not be considered conclusive, used to inform clinical practice,
or referenced by the media as validated information.

Rutin Attenuates Liver Fibrosis by the IRG1-Itaconate-Nrf2 Axis: Modulation of Oxidative Stress and NLRP3 Inflammasome Activation

Ningman Jiang
The First Affiliated Hospital of Chongqing Medical University,
Jiao Zhang
Chongqing Medical University
Ge Kuang
Chongqing Medical University
Guohao Liu
Chongqing Medical University
Jingyuan Wan
Chongqing Medical University
Bin wang
The First Affiliated Hospital of Chongqing Medical University,
Zizuo Zhao
zhaozz513@hospital.cqmu.edu.cn

The First Affiliated Hospital of Chongqing Medical University,

Research Article

Keywords: Rutin, liver fibrosis, IRG1, itaconate, oxidative stress, NLRP3 inflammasome

Posted Date: March 24th, 2026

DOI: https://doi.org/10.21203/rs.3.rs-8939517/v1

License: This work is licensed under a Creative Commons Attribution 4.0 International License.
Read Full License

Additional Declarations: No competing interests reported.

Version of Record: A version of this preprint was published at Inflammation Research on June 20th, 2026. See the published version at https://doi.org/10.1007/s00011-026-02298-3.

Abstract

Liver fibrosis, a common outcome of chronic liver injury, is characterized by excessive inflammation and oxidative stress. Rutin, a bioactive flavonoid with known antioxidant and anti-inflammatory properties, has not been thoroughly investigated for its potential anti-fibrotic mechanisms. This study aimed to elucidate the role of Rutin in liver fibrosis and its underlying molecular pathways. A carbon tetrachloride (CCl_4)-induced murine liver fibrosis model was employed. Liver injury, fibrotic deposition, inflammatory response, and oxidative stress were evaluated through histopathological examination, Western blotting, quantitative real-time PCR, and RNA sequence. The involvement of immune-responsive gene 1 (IRG1) was investigated using IRG1-knockout mice, while molecular docking and cellular thermal shift assay (CETSA) were performed to assess Rutin-IRG1 binding. The results showed that Rutin treatment significantly attenuated CCl_4-induced hepatic injury and collagen accumulation, accompanied by reduced markers of fibrosis. Mechanistically, Rutin activated the IRG1-itaconate axis, leading to a notable decrease in reactive oxygen species and pro-inflammatory cytokine release by Nrf2 activation and NLRP3 inflammasome containment. Molecular analyses confirmed direct binding of Rutin to IRG1, stabilizing its structure and enhancing its functional activity. The protective effects of Rutin were abolished in IRG1-deficient mice, underscoring the essential role of IRG1 in its anti-fibrotic action. In conclusion, Rutin ameliorates liver fibrosis by mitigating oxidative stress and suppressing NLRP3 inflammasome activation through targeting the IRG1/itaconate pathway, revealing a novel immunometabolic mechanism for its hepatoprotective effect.

Introduction

Liver fibrosis occurs primarily in chronic liver disease **with** chronic hepatocyte damage, iterative liver inflammation, excessive oxidative stress and persistent activation of hepatic fibrogenesis. These chronic liver diseases are caused by a variety of etiologies including viral liver disease, alcoholic liver disease, non-alcoholic fatty liver disease and autoimmune liver diseases [1] . Liver fibrosis is curable and reversible, but it is irreversible when progress to cirrhosis or even hepatocellular carcinoma [2, 3]. Currently, liver transplantation is the most effective treatment for liver fibrosis. However, because of the scarcity of organ donors, its clinical application is not popular. Herein, finding promising agents to alleviate liver dysfunction and decrease complications is necessary for liver fibrosis management.

It has been widely accepted that oxidative stress and inflammation play critical roles in liver fibrosis [4]. When continuously stimulated by a variety of pathogenic factors, the balance of oxidative stress in the liver is broken, and the liver releases a large number of oxygen free radicals and reactive oxygen species (ROS), which induce hepatocyte injury and death. Dying hepatocytes release damage-associated molecular patterns (DAMPs) that are recognized by pattern recognition receptor (PRR), further activate innate immune signals including Nuclear Factor kappa-light-chain-enhancer of activated B cells (NF-κB) and inflammasome NOD-like receptor pyrin domain-containing 3 (NLRP3), resulting in the production and release of numerous inflammatory signals including cytokines, chemokines and neutrophil-mediated ROS [5-7]. This, in turn, promotes apoptosis and necrosis of hepatocytes, forming a feedforward loop of

oxidative stress-inflammation-cell death [7] . Meanwhile, ROS and inflammatory signals such as transforming growth factor beta 1 (TGF-β1), tumor necrosis factor-α (TNF-α) and interleukin-1β (IL-1β) activate hepatic stellate cell (HSC), resulting in excessive collagen deposition in the extracellular matrix (ECM), leading to liver fibrosis [8-11] .

Endogenous complex anti-inflammatory and antioxidant defense systems also exist in the liver, which are regulated by a series of pathways to ensure that the response to inflammation and ROS is sufficient to meet the body's needs [12]. Itaconate is a regulatory metabolite in the tricarboxylic acid (TCA) cycle, and it also acts as an immunomodulator. It is synthesized by cis-aconitic acid, a TCA cycle intermediate, and catalyzed by cis-aconitic acid decarboxylase encoded by the immune response gene 1 protein (IRG1) [13]. Recently, itaconate has received considerable attention due to its critical role in negatively regulating inflammatory responses and cytokine production as an anti-inflammatory metabolite [14, 15]. Nuclear factor E2-related factor 2 (Nrf2), a ubiquitous transcription factor, is the master antioxidant regulator for cells to cope with oxidative stress. The fundamental and induced expression of a string of antioxidant response element-dependent genes including heme oxygenase-1 (HO-1) and quinone oxidoreductase 1 (NQO1), are driven by Nrf2 to regulate the physiological and pathophysiological consequence of oxidant exposure [16, 17]. Previous studies had shown a link between the IRG1/itaconate pathway and Nrf2, and a recent study using IRG1$^{-/-}$mice demonstrated that IRG1 suppresses injury and inflammation during hepatic ischemia-reperfusion (I/R), and that the mechanism of the itaconate derivative 4-octyl itaconate (4-OI) protected against hepatic I/R injury requires Nrf2 [18].

Rutin, known as quercetin-3-O-Rutinoside and vitamin P, is a polyphenolic natural flavonoid originated from many medicinal plants and vegetables[19]. Its chemical structure was identified as (2-(3,4-dihydroxyphenyl)-4,5-dihydroxy-3-[3,4,5trihydroxy-6-[(3,4,5-trihydroxy-6methyl-oxan-2-yl) oxymethyl] oxan-2-yl] oxy -chromen-7-one (Fig. 1A) [20]. It is reported that Rutin shows a wide range of pharmacological/biological activities including antioxidant, anti-inflammatory, hepatoprotective and neuroprotective effects [21-25]. Previous studies had shown Rutin had hepatoprotection on liver injury induced by different models, including bile duct ligation and high-fat diet [23, 25]. However, there is little research on the therapeutic effect of Rutin on hepatic fibrosis, and the potential molecular mechanism remains undefined.

In this study, we explored that whether Rutin had protective effects in CCl_4-induced liver fibrosis model and whether these protective effects were related to its anti-inflammatory, antioxidant properties and IRG1-itaconate pathway.

Materials and Methods

Animals and Experimental Design

IRG1 knockout (KO, IRG1$^{-/-}$) mice (Cyagen, S-KO-02679) and their C57BL/6N cognate background control mice were bred and raised under specific pathogen-free conditions. All mice were 8-12 weeks old

male mice weighing 20-30 g, housed in standard laboratory animal cages and maintained with standard management conditions of a 12 h light/ dark cycle. All experimental procedures were approved by the ethics committee of Chongqing Medical University, and conducted in accordance with the ARRIVE guidelines and the national research council's guide for the care and use of laboratory animals.

To explore the effect of Rutin dose on its biological effects, all mice were randomly divided into six groups. (1) Vehicle control, (2) Rutin, (3) CCl_4, (4) CCl_4+Rutin (15 mg/kg), (5) CCl_4+Rutin (30 mg/kg), (6) CCl_4+Rutin (60 mg/kg). To investigate the protective mechanism of Rutin against liver fibrosis, WT mice and $IRG1^{-/-}$ mice were used in CCl_4 group or CCl_4+Rutin (60 mg/kg) group. Rutin (suspended in 0.1% CMC-Na) was intragastrically (i.g.) administered to corresponding group of mice for 10 consecutive days. Vehicle groups of mice received corresponding volume of CMC-Na solution. Hepatic fibrosis was induced by intraperitoneal (i.p.) injections of CCl_4 (0.5 ml/kg, dissolved in olive oil, 1:19) three times a week for 8 weeks. Same volume of olive oil was injected to the normal control group. All mice were sacrificed 48 h after final CCl_4 injection. All serum samples and liver samples were collected for further examination.

Biochemical Assay

Blood samples were collected through retro-orbital bleeding. The serum samples were obtained by centrifugation at 3600 rpm for 10 min at 4°C. Serum enzyme activities of alanine aminotransferase (ALT) and aspartate aminotransferase (AST) were measured by spectrophotometry using corresponding detection kits (Nan Jing Jan Cheng Biochemical Institute, Nanjing, China) according to the instruction.

Histologic Analysis

Some excised liver specimens were fixed with 4% paraformaldehyde solution and then embedded in paraffin. Paraffin sections were stained with hematoxylin and eosin (H&E), and then were scored using the Suzuki methodology to assess tissue inflammation and necrosis. Sirius red staining and Masson staining were performed in paraffin sections according to standard protocol.

Detection of Tissue ROS

Some liver samples were snap frozen in liquid nitrogen and kept at -80°C. To determine the hepatic ROS levels, the frozen liver samples were sectioned transversely. The 10 μm thick of frozen liver section was treated with 10 μmol/L fluorescent dye dihydroethidium (DHE) and incubated at 37°C for 30 min in the dark. Then the nuclei were stained with DAPI and the fluorescence images were obtained by fluorescence microscope (Nikon, Tokyo, Japan).

Measurement of Peroxidation

The peroxidation products of various biomacromolecules in liver tissue were detected, including the lipid peroxidation product 4-HNE, the protein peroxidation products Protein Carbonyl and the nucleic acid

peroxidation products 8-OHG, 8-OHdG and 8-hydroxyguanine. The production of 4-HNE was demonstrated by immunohistochemistry, and the contents of protein carbonyl and 8-OHG, 8-OHdG, 8-hydroxyguanine were measured by ELISA. The specific methods are in 2.9 and 2.10.

Examination for Antioxidant Enzymes

Commercially available assay kits for the examination of hepatic superoxide dismutase (SOD) and catalase (CAT) activities were obtained from Nan Jing Jan Cheng Biochemical Institute (Nanjing, China). The activity of SOD was determined by colorimetry. The principle, briefly, is that superoxide anions ($O_2^{\bullet -}$) are produced by xanthine and xanthine oxidase reaction systems, which reduce WST-1 to orange or purple WST-1 Formazan dye. The reactions of CAT decomposing H_2O_2 are quickly terminated by adding ammonium molybdate and the remaining H_2O_2 reacts with ammonium molybdate to produce a pale-yellow complex. The activity of CAT can be calculated by measuring its change at 405 nm.

Hydroxyproline (Hyp) Assay

The level of Hepatic Hyp was examined by using the corresponding kit (Nan Jing Jan Cheng Biochemical Institute, Nanjing, China) according to the supplier's protocol. The oxidation product of hydroxyproline reacts with dimethylaminobenzaldehyde to form a purple complex, and the level of Hyp can be calculated by colorimetry.

Reverse Transcription-Quantitative Polymerase Chain Reaction (RT-qPCR) and RNA Sequencing

The total RNA of liver tissues was extracted using Trizol reagent. Then, NanoDrop One microvolume spectrophotometer was used to quantify total RNA. Equal amount of RNA was reversibly transcribed into complementary DNA. PCR reactions were used to amplify the target gene. Its procedure, briefly, consisted of starting at 94°C for 5 min, followed by 32-40 cycles of amplification (denaturation at 94°C for 1 min, annealing at 58°C for 30 s, and extension at 72°C for 30 s) with a final primer extra-extension at 72°C for 7 min. The PCR products were separated on 2% agarose gel and stained with ethidium bromide. The intensity of each target gene mRNA band was quantified by molecular imaging system and β-actin was used as internal control. The sequences of the primers are listed in **Table 1**.

Tissue Preparation and Western Blot Analysis

Liver tissue removed from -80°C, triturated and lysed in RIPA lysis buffer containing protease inhibitors. Total protein concentrations were measured with BCA kit and normalized with buffer. Then, proteins were electrophoretically separated by SDS-PAGE and transferred to polyvinylidene fluoride membranes. After blocking with 5% nonfat dry milk for 1 h, the membranes were incubated overnight with the indicated antibodies (IRG1, NQO1, HO-1, NLRP3, ASC, pro-caspase1, TLR4, IκB, p65) in 4°C. Membranes were incubated with horseradish peroxidase-conjugated secondary antibodies for 1 h, then visualized by chemiluminescence (Bio-Rad).

Immunohistochemical and Immunofluorescence Staining

Paraffin sections were used for immunohistochemical staining. They were deparaffinized, hydrated and incubated with H_2O_2 to block endogenous peroxidase. After retrieved by microwave and blocked with 5% BSA, the liver sections were incubated with primary antibody overnight at 4°C. Sections were then co-incubated with biotinylated secondary antibodies for 1 h, followed by avidin-biotin-peroxidase complexes. The immunoreactive signal is generated by color deposition with diaminobenzidine as a substrate.

For immunofluorescence staining, the frozen sections were washed in TBS, and then blocked in 5% BSA for 1 h. Following overnight incubation with primary antibodies, the corresponding fluorescent-labeled secondary antibodies were applied. DAPI dye was used to stain the nuclei. After mounting with anti-quenching fluorescent mounting medium, images were obtained using a fluorescence microscope (Leica, USA).

Enzyme-Linked ImmunoSorbent Assay (ELISA)

The levels of cytokines, chemokines and peroxidation products in liver cell supernatants were measured using ELISA Bender medsystems kits according to the manufacturer's instructions.

Measurements of Itaconate

Samples were injected by Thermo Fisher Vanquish ultra-high-performance liquid chromatography (HPLC) and separated over a reversed-phase Thermo Fisher Hypercarb porous graphitic column maintaining at 52°C. The mobile phase contains solvent A (0.1% formic acid in water) and solvent B (0.1% formic acid in acetonitrile). Itaconate concentrations were quantified using liquid chromatography-mass spectrometry analysis. Deuterated (D4)-taurine and (D3)-lactate (Sigma-Aldrich) were used as an internal standard.

Molecular Docking and Dynamics Simulations

The molecular docking study was performed to explore the binding mode and affinity between Rutin and the IRG1 protein. The three-dimensional crystal structure of human IRG1 was retrieved from the Protein Data Bank. Docking was carried out with *AutoDock4* software. The IRG1 protein was defined as the rigid receptor, while all rotatable bonds in Rutin were set as flexible. Ten independent docking runs were performed, and the resulting poses were ranked according to their binding affinity (kcal/mol). The pose with the lowest binding energy and highest cluster occupancy was selected for further analysis. Visualization and interaction analysis (hydrogen bonds, hydrophobic contacts) were conducted using *Pymol2 software*.

To evaluate the stability and dynamic behavior of the Rutin-IRG1 complex, molecular dynamics (MD) simulations were performed using the GROMACS package. The complex obtained from molecular docking was solvated in a cubic water box. Production MD simulation was then carried out for 100 ns under periodic boundary conditions. The algorithm constrained bond lengths, and the Particle Mesh Ewald method was used for long-range electrostatic interactions. Trajectories were analyzed for root

mean square deviation (RMSD), root mean square fluctuation (RMSF), radius of gyration (Rg), solvent-accessible surface area (SASA), and hydrogen bond occupancy. The binding free energy was calculated.

Cellular Thermal Shift Assay (CETSA)

The Cellular Thermal Shift Assay was employed to validate the direct binding between Rutin and the intracellular target IRG1 in a cellular context. HepG2 cells were seeded in 6-well plates and allowed to adhere overnight. Cells were then treated with either Rutin (10 μM) or an equivalent volume of vehicle control (DMSO). Following treatment, cells were harvested, washed with PBS, and resuspended. The cell suspension was aliquoted into PCR tubes and heated at a gradient of temperatures (ranging from 37°C to 67°C) for 3 minutes in a thermal cycler, followed by incubation at room temperature for an additional 3 minutes. Cells were then subjected to three freeze-thaw cycles using liquid nitrogen to lyse the cells. The soluble protein fraction was separated from cell debris by centrifugation at 12,000 × g for 15 minutes at 4°C. The supernatant was collected, and the protein concentration was determined. Equal amounts of protein from each temperature point were resolved by SDS-PAGE, followed by Western blotting analysis using a specific anti-IRG1 antibody. The band intensity of soluble IRG1 remaining at each temperature was quantified using ImageJ software.

Statistical Analyses

These data were expressed as mean ± SD. Statistical analysis was carried out using one-way or two-way ANOVA followed by a Bonferoni comparison or Dunnett's multiple comparison test to determine the differences among groups. $P< 0.05$ was considered as statistically significant.

Results

Rutin Attenuates CCl_4-Induced Liver Injury and Fibrosis in Mice

Rutin exhibited significant hepatoprotective and antifibrotic effects in a mouse model of CCl_4-induced liver injury. Its characteristic flavonoid molecular structure underlies its notable bioactivity (**Fig. 1A**). Biochemical assays showed that CCl_4 administration markedly elevated AST and ALT levels, indicating hepatocellular injury, whereas Rutin treatment significantly reduced these enzyme levels (**Fig. 1B, 1C**). Histopathological examination using H&E staining revealed that CCl_4 disrupted hepatic lobular architecture, caused hepatocellular swelling, collagen deposition, and substantial inflammatory infiltration, all of which were alleviated in a dose-dependent manner by Rutin (**Fig. 1D**). In the context of liver fibrosis, Masson's trichrome and Sirius Red staining demonstrated excessive collagen accumulation in CCl_4-treated livers, which was significantly reduced following Rutin administration (**Fig. 1E, 1F**). Consistently, hepatic hydroxyproline content was elevated in the CCl_4 group and markedly decreased in the Rutin-treated groups (**Fig. 1G**). Immunohistochemical analyses further revealed that CCl_4 induced strong α-smooth muscle actin (α-SMA) and type I collagen alpha 1 (Col1a1) expression in the periportal region, reflecting HSC activation and fibrogenesis, both of which were significantly attenuated by Rutin (**Fig. 1H, 1I**). RT-qPCR analysis confirmed that CCl_4 markedly upregulated the mRNA expression of

fibrosis-related genes, including Col1a1, CTGF, TGF-β, and TIMP-1, while Rutin treatment significantly suppressed these transcriptional changes (**Fig. 1J–1M**). Together, these results show that Rutin attenuates CCl_4-induced liver injury and fibrosis, as evidenced by reduced serum transaminase levels, improved histological architecture, decreased collagen deposition, and suppression of fibrotic marker expression.

Rutin Attenuates CCl_4-Induced Hepatic Inflammation and Oxidative Stress in Mice

To comprehensively elucidate the anti-inflammatory and antioxidant effects of Rutin in a CCl_4-induced mouse model of liver injury, we conducted a series of analyses at multiple levels, including gene expression, immune cell infiltration, oxidative damage markers, and antioxidant enzyme activity. RT-qPCR analysis demonstrated that Rutin treatment significantly downregulated the hepatic mRNA expression of pro-inflammatory cytokines IL-6 and TNF-α, as well as chemokines CCL2 and CXCL1 (**Fig. 2A–2D**), indicating its potent anti-inflammatory capacity. Immunofluorescence staining further revealed that CCl_4 exposure markedly increased the infiltration of F4/80-positive macrophages and CD11b-positive neutrophils in liver tissue, which was notably alleviated by Rutin administration (**Fig. 2E, 2F**), suggesting an inhibitory effect on inflammatory cell recruitment. Regarding oxidative stress, immunohistochemical staining showed a substantial elevation of the lipid peroxidation marker 4-hydroxynonenal (4-HNE) following CCl_4 treatment, which was significantly reduced upon Rutin intervention (**Fig. 2G**). ELISA assays confirmed that CCl_4 induced a marked increase in hepatic levels of oxidative damage markers, including the protein peroxidation product protein carbonyl and nucleic acid oxidation products 8-OHG, 8-OHdG, and 8-hydroxyguanine, all of which were significantly attenuated by Rutin (**Fig. 2H, 2I**). Furthermore, enzymatic activity assays showed that CCl_4 markedly suppressed the hepatic activities of key antioxidant enzymes SOD and CAT, while Rutin treatment effectively restored their activity levels (**Fig. 2J, 2K**). These results indicate that Rutin reduces hepatic inflammation and oxidative stress in CCl_4-treated mice, as evidenced by decreased pro-inflammatory cytokine expression, reduced immune cell infiltration, lower oxidative damage markers, and restored antioxidant enzyme activity.

Rutin Activates the Nrf2 Pathway and Inhibits the NLRP3–NF-κB Axis in the Liver of CCl_4-Treated Mice

Rutin exerts significant regulatory effects on oxidative stress and inflammatory signaling pathways in the liver. Specifically, Rutin treatment markedly upregulated the expression of Nrf2 and its downstream antioxidant enzymes NQO1 and HO-1 in the liver of CCl_4-treated mice (**Fig. 3A**), which was further confirmed by semi-quantitative Western blot analysis showing consistent increases in the protein levels of Nrf2, NQO1, and HO-1 (**Fig. 3B–3D**), suggesting that Rutin enhances hepatic antioxidant defense via activation of the Nrf2 pathway. Conversely, the expression of NLRP3 and its downstream signaling molecules ASC and pro-caspase-1, which were significantly induced by CCl_4, were markedly reduced following Rutin administration (**Fig. 3E**). This inhibitory effect was further supported by Western blot analysis, which demonstrated consistent downregulation of NLRP3, ASC, caspase-1, and IL-1β protein levels (**Fig. 3F–3I**). Additionally, Western blot analysis revealed that CCl_4 markedly activated the NF-κB signaling pathway, as evidenced by elevated expression of TLR4, p-IκB, and p-p65, whereas Rutin

effectively suppressed these changes (**Fig. 3J**) and the semi-quantitative analysis of NLRP3, ASC, caspase-1, and IL-1β protein levels confirmed this trend (**Fig. 3K–3N**). Furthermore, HPLC analysis demonstrated that Rutin significantly increased the hepatic content of itaconate in CCl_4-treated mice (**Fig. 3O**), indicating a potential involvement of endogenous immunometabolic regulation in its anti-inflammatory and antioxidant effects. These results show that Rutin upregulates the hepatic Nrf2 pathway and its downstream antioxidant enzymes, while suppressing the NLRP3 inflammasome and NF-κB signaling activation induced by CCl_4. Additionally, Rutin increases hepatic itaconate levels, suggesting involvement of endogenous metabolic regulation in these responses.

Molecular interactions between Rutin and IRG1

This study investigates the interactions between Rutin and IRG1 through molecular docking and molecular dynamics (MD) simulations. Molecular docking results show that Rutin forms hydrogen bonds with several amino acids of IRG1, including ASN-425, ILE-347, ASP-285, ARG-273, and ASP-417, enhancing binding affinity. Additionally, Rutin interacts with ARG-273 through cation-π conjugation and strengthens the binding further through hydrophobic interactions with ARG-273, VAL-349, LYS-421, and ALA-424 (**Fig. 4A**). MD simulation reveals that the RMSD of the complex quickly reaches equilibrium within 0–10 ns (around 1.2 Å), then gradually increases to 2.0 Å between 40–60 ns, rising sharply to 3.5 Å at 60 ns, and stabilizing at approximately 3.0 Å, indicating the system reaches a new equilibrium state (**Fig. 4B**). RMSF analysis shows that the protein's flexibility decreases, with values generally below 2 Å, indicating rigidity in the protein core, which supports stable binding and enzymatic activity (**Fig. 4C**). RoG analysis shows slight conformational relaxation between 0–20 ns, with RoG increasing from 22.2 Å to 22.5 Å, and stabilizing between 22.6–22.7 Å after a significant increase at 60 ns, indicating a new equilibrium state (**Fig. 4D**). MM-GBSA calculations show a binding energy of -16.38±4.79 kcal/mol, indicating strong binding affinity, primarily driven by electrostatic and van der Waals interactions (**Fig. 4E**). Energy decomposition identifies key amino acids contributing to binding, such as GLU 297, ALA 296, and VAL 295 (**Fig. 4F**). Hydrogen bond analysis shows an initial increase to 10 bonds, followed by a drop to zero between 20–60 ns, and a recovery to 2–6 bonds between 60–100 ns, suggesting conformational shifts and a new interaction equilibrium (**Fig. 4G**). and CETSA analysis showed that Rutin significantly enhances IRG1 thermal stability (**Fig. 4H**). These findings indicate that Rutin binds IRG1 through multiple stable interactions and induces conformational stabilization of the protein. This structural basis supports a potential role for Rutin in modulating IRG1 function at the molecular level.

IRG1 Deficiency Abolishes Rutin-Mediated Activation of Nrf2 and Inhibition of NF-κB Signaling

To further investigate whether the antifibrotic effect of Rutin is dependent on the IRG1 pathway, we established an $IRG1^{-/-}$ mouse model of CCl_4-induced liver fibrosis. Western blot analysis revealed that Rutin markedly upregulated the protein expression of Nrf2 and its downstream antioxidant enzymes NQO1 and HO-1 in liver tissue; however, this upregulation was significantly attenuated in IRG1-deficient mice (**Fig. 5A**), and semi-quantitative analysis showed consistent trends for Nrf2, NQO1, and HO-1 levels (**Fig. 5B–5D**), suggesting that IRG1 plays a crucial role in mediating Rutin-induced activation of the Nrf2

pathway. Similarly, in WT mice, Rutin significantly inhibited the CCl_4-induced expression of NLRP3 inflammasome-related proteins, including NLRP3, ASC, Caspase-1, and IL-1β, whereas this inhibitory effect was markedly diminished in IRG1$^{-/-}$ mice (**Fig. 5E**), which was further supported by Western blot semi-quantitative analysis (**Fig. 5F–5I**), indicating a potential involvement of IRG1 in the negative regulation of inflammasome activation by Rutin. In addition, Western blot results showed that CCl_4 administration significantly activated the NF-κB signaling pathway, as evidenced by elevated protein levels of TLR4, p-IκB, and p-p65 in the liver, and these increases were effectively suppressed by Rutin in WT mice but not in IRG1$^{-/-}$ mice (**Fig. 5J**); consistent trends were observed in the semi-quantitative analysis of TLR4, p-IκB, IκB, p-p65, and p65 expression levels (**Fig. 5K–5N**), further supporting the role of IRG1 in Rutin-mediated inhibition of NF-κB activation. Notably, HPLC analysis demonstrated that Rutin significantly increased hepatic itaconate content in CCl_4-treated WT mice, while this elevation was abolished in IRG1$^{-/-}$ mice (**Fig. 5O**), further supporting the hypothesis that Rutin exerts its anti-inflammatory and antioxidant effects, at least in part, through the IRG1/itaconate metabolic pathway. These findings indicate that the presence of IRG1 is essential for Rutin to exert its regulatory effects on the Nrf2 antioxidant response and the NLRP3–NF-κB inflammatory axis, highlighting the importance of the IRG1/itaconate pathway in the hepatoprotective mechanism of Rutin.

IRG1 Deficiency Attenuates the Anti-inflammatory and Antioxidant Effects of Rutin in CCl_4-Induced Liver Injury

In the context of IRG1 gene knockout, we further evaluated hepatic inflammation and antioxidant responses to determine whether the anti-inflammatory and antioxidant effects of Rutin are mediated through the IRG1 pathway. RT-qPCR analysis revealed that Rutin significantly downregulated the mRNA expression of pro-inflammatory cytokines IL-6 and TNF-α, as well as chemokines CCL2 and CXCL1 in the liver of CCl_4-treated mice, indicating a potent anti-inflammatory effect. However, this inhibitory effect was markedly attenuated in IRG1$^{-/-}$ mice (**Fig. 6A–6D**). Consistently, immunofluorescence staining showed that CCl_4 exposure significantly increased the hepatic infiltration of F4/80-positive macrophages and CD11b-positive neutrophils, which was notably reduced by Rutin treatment in wild-type mice but not in IRG1-deficient mice (**Fig. 6E, 6F**). Regarding oxidative stress, immunohistochemical analysis demonstrated that hepatic levels of the lipid peroxidation marker 4-HNE were significantly elevated following CCl_4 exposure, whereas Rutin administration markedly reduced 4-HNE accumulation; this reduction was impaired in IRG1$^{-/-}$ mice (**Fig. 6G**). ELISA further confirmed that the levels of hepatic oxidative damage markers, including the protein peroxidation product protein carbonyl and nucleic acid oxidation products 8-OHG, 8-OHdG, and 8-hydroxyguanine, were significantly increased in CCl_4-treated mice and effectively attenuated by Rutin, whereas these protective effects were substantially diminished in IRG1$^{-/-}$ mice (**Fig. 6H, 6I**). Additionally, enzymatic activity assays revealed that CCl_4 significantly suppressed the hepatic activities of the key antioxidant enzymes SOD and CAT, which were restored by Rutin treatment in wild-type mice, but this restoration was abolished in IRG1-deficient mice (**Fig. 6J, 6K**). These findings indicate that IRG1 plays a critical regulatory role in the anti-inflammatory and antioxidant effects of Rutin, and that the absence of IRG1 significantly compromises the hepatoprotective efficacy of

Rutin, highlighting the IRG1/itaconate pathway as a potential mechanistic basis for its therapeutic actions.

IRG1 Deficiency Impairs the Hepatoprotective and Antifibrotic Effects of Rutin in CCl_4-Induced Liver Injury

In the context of IRG1 gene deficiency, we further evaluated hepatic injury and fibrosis to determine whether the protective effects of Rutin against tissue damage and fibrosis are associated with the IRG1 pathway. Biochemical analysis revealed that CCl_4 administration significantly elevated serum levels of AST and ALT, indicating hepatocellular injury, whereas Rutin treatment markedly reduced these enzyme levels. However, this hepatoprotective effect was substantially attenuated in IRG1$^{-/-}$ mice (**Fig. 7A, 7B**). Histopathological examination using H&E staining demonstrated that CCl_4 disrupted hepatic lobular architecture, causing hepatocyte swelling, collagen deposition, and extensive inflammatory infiltration, all of which were alleviated by Rutin, while this improvement was significantly impaired in IRG1$^{-/-}$ mice (**Fig. 7C**). In the context of liver fibrosis, Masson's trichrome and Sirius Red staining revealed excessive collagen accumulation in the liver following CCl_4 exposure, which was markedly reduced by Rutin treatment in wild-type mice but not in IRG1-deficient mice (**Fig. 7D, 7E**). Consistently, hepatic hydroxyproline content, which was elevated after CCl_4 treatment, was significantly reduced by Rutin, whereas this effect was blunted in IRG1$^{-/-}$ mice (**Fig. 7F**). Immunohistochemical analysis further showed that CCl_4 induced strong perivascular expression of α-SMA and Col1a1, reflecting hepatic stellate cell activation and fibrogenesis, both of which were significantly attenuated by Rutin in wild-type mice but not in IRG1-deficient mice (**Fig. 7G, 7H**). Moreover, RT-qPCR analysis confirmed that CCl_4 markedly upregulated the mRNA expression of fibrosis-related genes, including Col1a1, CTGF, TGF-β, and TIMP-1, and these transcriptional changes were significantly suppressed by Rutin, while this suppressive effect was abolished in IRG1$^{-/-}$ mice (**Fig. 7I-7L**). These findings indicate that IRG1 plays a critical role in mediating the protective effects of Rutin against CCl_4-induced hepatic injury and fibrosis, highlighting the IRG1/itaconate pathway as a potential mechanistic basis for its antifibrotic activity.

Discussion

CCl_4 has been widely used to induce liver injury and fibrosis in mice [26]. CCl_4 is one of halogenated alkanes that activated by cytochrome (CYP)2E1 to form a highly reactive trichloromethyl radical and promote excessive generation of ROS. The trichloromethyl radical and its peroxy radical $CCl_3OO^{\bullet-}$ are involved in lipid peroxidation processes and several free radical reactions that contribute to the activation of Kupffer cells and the induction of an inflammatory response [27, 28]. Kupffer cells activated by CCl_4 release TNF-α, TGF-β, and IL-1, IL-6, and IL-10. HSCs activated by CCl_4 and inflammatory mediators over-produce type-I collagen, and thus promote liver fibrosis. In brief, CCl_4-induced fibrosis is closely related to oxidative stress and inflammation. In our study, Rutin was found to inhibit CCl_4-induced liver inflammation and oxidative stress. Rutin might be a potent agent to treat liver fibrosis owing to its antioxidant and anti-inflammatory biological activities.

Oxidative stress is closely associated with the progress of CCl_4-induced liver injury and fibrosis. CCl_4-induced increase in hepatic ROS level. Several studies had shown that ROS played an important role in the regulation of HSCs activation and fibrotic gene expression [29]. After activated by ROS, HSCs proliferate and excessively release collagen into the ECM propagating liver fibrosis. The excessive ROS can also activate the lipid peroxidation of hepatocytes to cause the increase generation of lipid peroxides including 4-HNE, which easily modify proteins and inhibit critical enzyme activities. Antioxidant enzymes, especially SOD and CAT, can reduce the level of superoxide (O_2^-) and hydrogen peroxide (H_2O_2), which are the most-produced ROS [30]. Nrf2 is one of master regulators to cope with oxidative stress. In the oxidatively stimulated state, Nrf2 remains stable and enters the nucleus, where it binds to antioxidant response elements, resulting in transcriptional activation of genes encoding a series of antioxidant enzymes, including HO-1 and NQO1, to restore redox homeostasis in the body [31-35]. For these reasons, we observed the helpful effect of Rutin on CCl_4-induced liver injury and fibrosis by detecting hepatic ROS level, production of lipid peroxidation products, antioxidant enzyme activities and Nrf2 pathway. The results showed that Rutin could significantly reduce the hepatic ROS level, decrease the production of 4-HNE, and increase the activities of SOD and CAT, and activation of Nrf2 pathway, suggesting that the protective effect of Rutin on liver injury and fibrosis might be associated with its antioxidant activity.

Inflammation is another critical pathological mechanism promoting CCl_4-induced liver injury and fibrosis. DAMPs released from damaged or dying hepatocytes are recognized by PRRs on Kupffer cells and further activate Kupffer cells [36] . Activated kupffer cells produce cytokines and chemokines including IL-1β, IL-6, TNF-α, CCL2 and CXCL1, participate in the inflammatory response and induce the activation of HSCs [11]. IL-1β is a main pro-inflammatory cytokine produced during NLRP3 inflammasome activation. TNF-α is considered to be the main endogenous harmful mediator during liver injury, which has the ability to directly damage tissues and trigger inflammatory cascades [37]. IL-6 is another pro-inflammatory cytokine that antagonizes TNF-α-induced tissue damage. In this study, Rutin decreased the mRNA and protein levels of IL-1β, IL-6, TNF-α in CCl_4-treated mice. The release of chemokines such as CCL2 and CXCL1 recruit macrophages and neutrophils to participate in the initial stage of inflammatory response in the process of liver fibrosis. In our results, we observed Rutin sharply decreased the mRNA and protein levels of CCL2 and CXCL1 in CCl_4-treated mice. In addition, we found aggregation of macrophages and neutrophils in the liver of mice following CCl_4 administration, whereas Rutin treatment significantly reduced this activity. Previous studies have demonstrated that inhibition of NLRP3 inflammasome ameliorates CCl_4-induced liver fibrosis [38-41]. ASC and pro-caspase 1 are key components of NLRP3 inflammasome [42, 43]. In the present study, the decline of NLRP3, ASC and pro-caspase 1 protein levels was observed in CCl_4 mice after Rutin treatment. TLR4 is a critical PRR involved in the triggering of CCl_4-induced cascades of inflammatory responses. NF-κB is a classic inflammatory signaling pathway that promotes the occurrence of inflammatory responses, of which IkB and p65 are important components of this pathway [11]. It has been reported that the knockout of TLR4 can alleviate inflammatory response to attenuate CCl_4-induced hydroxyproline and α-SMA [44]. In the present study,

Rutin was observed to decrease the level of TLR4 and the phosphorylation of IκB and p65 in the liver of CCl_4-treated mice. These results suggest that Rutin inhibits liver inflammation by inhibiting the activation of NF-κB and inflammasome NLRP3 signaling pathways after CCl_4 exposure.

To sum up, Rutin inhibits hepatic oxidative stress by promoting Nrf2 signaling, and inhibits hepatic inflammation by inhibiting the activation of NF-κB and inflammasome NLRP3 signaling pathways, so we speculate whether there is an intermediate molecule affected by Rutin, which is involved in the regulation of the above signaling pathways. Itaconate, an endogenous biological metabolite catalyzed by IRG1 and accumulated by metabolic disorders after inflammatory activation of macrophages, is also acts as an immunomodulator. Previous study had shown a link between the IRG1/itaconate pathway and Nrf2, when itaconate was shown to directly alkylate cysteine residues in Kelch-like ECH-associated protein 1 (Keap1), leading to an increase in Nrf2 in macrophages during endotoxemia [45]. Endogenous itaconate and its derivative 4-OI have been presented to alkylate cysteine residues on plenty of proteins, including Keap1, and this form of cysteine alkylation, called 2, 3-dicarboxypropylation or itaconation, has been exhibited to be a crucial component involved in the anti-inflammatory properties of itaconate [46-48]. In a recent study, 4-OI inhibited the inflammatory response by inhibiting NF-κB signal pathway in RAW264.7 cells[49]. A previous study has reported that itaconate induced dicarboxypropylation of NLRP3 cysteine C548 and inhibited inflammasome activation, providing evidence that itaconate is a specific endogenous inhibitor of NLRP3 inflammasome activation [50]. We hypothesized that that Rutin further promotes Nrf2 pathway and inhibits NF-κB and inflammasome NLRP3 signaling pathways by regulating IRG1-itaconate axis. Therefore, we repeated the above experiments with $IRG1^{-/-}$ mice and found that the protective effect of Rutin on liver injury and fibrosis was weakened. It indicated that the protective effects of Rutin on CCl_4-induced liver injury and fibrosis was related to the IRG1-itaconate axis.

Conclusion

The results of this experiment support the hepatic beneficial effects of Rutin, and Rutin supplementation may reduce drug-induced liver injury and fibrosis in mice. We have demonstrated that Rutin has a certain inhibitory effect on CCl_4-induced liver injury, inflammatory response, oxidative stress and liver fibrosis in mice, possibly by further upregulating Nrf2 activity through IRG1-itaconate pathway and inhibiting inflammatory related pathways NLRP3 and NF-κB.

Abbreviations

ROS, reactive oxygen species; DAMPs, damage-associated molecular patterns; PRR, pattern recognition receptor; NF-κB, Nuclear Factor kappa-light-chain-enhancer of activated B cells; NLRP3, NOD-like receptor pyrin domain-containing 3; TGF-β1, transforming growth factor beta 1; TNF-α, tumor necrosis factor-α; IL-1β, interleukin-1β; ECM, extracellular matrix; TCA, tricarboxylic acid; IRG1, immune response gene 1 protein; Nrf2, Nuclear factor E2-related factor 2; HO-1, heme oxygenase-1; NQO1, quinone oxidoreductase 1; ALT, alanine aminotransferase; AST, aspartate aminotransferase; DHE,

Dihydroethidium; SOD, superoxide dismutase; CAT, Catalase; HPLC, high-performance liquid chromatography; HSC, hepatic stellate cell; O^{2-}, superoxide; H_2O_2, hydrogen peroxide.

Declarations

Acknowledgements

The study was supported by Chongqing Natural Science Foundation (CSTB2022NSCQ-MSX0061)

Declaration of competing interest

The authors declare that they have no known competing financial interests or personal relationships that could have appeared to influence the work reported in this paper.

Ethics Approval Animal studies were ethically approved by the Chongqing Medical University Ethics Committee (Certification Number:

20220305).

Data availability

Data will be made available upon request.

References

1. Parola M, Pinzani M. Liver fibrosis: Pathophysiology, pathogenetic targets and clinical issues. *Molecular aspects of medicine* 2019; 65:37-55.
2. Sun M, Kisseleva T. Reversibility of liver fibrosis. *Clin Res Hepatol Gastroenterol* 2015; 39 Suppl 1:S60-3.
3. Asrani SK, Devarbhavi H, Eaton J, Kamath PS. Burden of liver diseases in the world. *Journal of hepatology* 2019; 70:151-171.
4. Koyama Y, Brenner DA. Liver inflammation and fibrosis. *The Journal of clinical investigation* 2017; 127:55-64.
5. Chan JK, Roth J, Oppenheim JJ, Tracey KJ, Vogl T, Feldmann M, et al. Alarmins: awaiting a clinical response. *J Clin Invest* 2012; 122:2711-9.
6. Galluzzi L, Kepp O, Kroemer G. Mitochondria: master regulators of danger signalling. *Nat Rev Mol Cell Biol* 2012; 13:780-8.
7. Brenner C, Galluzzi L, Kepp O, Kroemer G. Decoding cell death signals in liver inflammation. *Journal of hepatology* 2013; 59:583-94.
8. Hernandez-Gea V, Friedman SL. Pathogenesis of liver fibrosis. *Annu Rev Pathol* 2011; 6:425-56.

9. Tsuchida T, Friedman SL. Mechanisms of hepatic stellate cell activation. *Nature reviews Gastroenterology & hepatology* 2017; 14:397-411.
10. Iwaisako K, Jiang C, Zhang M, Cong M, Moore-Morris TJ, Park TJ, et al. Origin of myofibroblasts in the fibrotic liver in mice. *Proceedings of the National Academy of Sciences of the United States of America* 2014; 111:E3297-305.
11. Kisseleva T, Brenner D. Molecular and cellular mechanisms of liver fibrosis and its regression. *Nature reviews Gastroenterology & hepatology* 2021; 18:151-166.
12. Jadeja RN, Upadhyay KK, Devkar RV, Khurana S. Naturally Occurring Nrf2 Activators: Potential in Treatment of Liver Injury. Oxid Med Cell Longev 2016; 2016:3453926.
13. Michelucci A, Cordes T, Ghelfi J, Pailot A, Reiling N, Goldmann O, et al. Immune-responsive gene 1 protein links metabolism to immunity by catalyzing itaconic acid production. *Proc Natl Acad Sci U S A* 2013; 110:7820-5.
14. Lampropoulou V, Sergushichev A, Bambouskova M, Nair S, Vincent EE, Loginicheva E, et al. Itaconate Links Inhibition of Succinate Dehydrogenase with Macrophage Metabolic Remodeling and Regulation of Inflammation. *Cell Metab* 2016; 24:158-66.
15. Bambouskova M, Gorvel L, Lampropoulou V, Sergushichev A, Loginicheva E, Johnson K, et al. Electrophilic properties of itaconate and derivatives regulate the IκBζ-ATF3 inflammatory axis. *Nature* 2018; 556:501-504.
16. Ma Q. Role of nrf2 in oxidative stress and toxicity. Annu Rev Pharmacol Toxicol 2013; 53:401-26.
17. Ross D, Siegel D. The diverse functionality of NQO1 and its roles in redox control. *Redox Biol* 2021; 41:101950.
18. Yi Z, Deng M, Scott MJ, Fu G, Loughran PA, Lei Z, et al. Immune-Responsive Gene 1/Itaconate Activates Nuclear Factor Erythroid 2-Related Factor 2 in Hepatocytes to Protect Against Liver Ischemia-Reperfusion Injury. *Hepatology* 2020; 72:1394-1411.
19. Negahdari R, Bohlouli S, Sharifi S, Maleki Dizaj S, Rahbar Saadat Y, Khezri K, et al. Therapeutic benefits of rutin and its nanoformulations. *Phytother Res* 2021; 35:1719-1738.
20. Calabrò ML, Tommasini S, Donato P, Stancanelli R, Raneri D, Catania S, et al. The rutin/beta-cyclodextrin interactions in fully aqueous solution: spectroscopic studies and biological assays. *J Pharm Biomed Anal* 2005; 36:1019-27.
21. Muvhulawa N, Dludla PV, Ziqubu K, Mthembu SXH, Mthiyane F, Nkambule BB, et al. Rutin ameliorates inflammation and improves metabolic function: A comprehensive analysis of scientific literature. *Pharmacol Res* 2022; 178:106163.
22. Tian C, Liu X, Chang Y, Wang R, Yang M, Liu M. Rutin prevents inflammation induced by lipopolysaccharide in RAW 264.7 cells via conquering the TLR4-MyD88-TRAF6-NF-κB signalling pathway. *J Pharm Pharmacol* 2021; 73:110-117.
23. AlSharari SD, Al-Rejaie SS, Abuohashish HM, Ahmed MM, Hafez MM. Rutin Attenuates Hepatotoxicity in High-Cholesterol-Diet-Fed Rats. Oxid Med Cell Longev 2016; 2016:5436745.

24. Enogieru AB, Haylett W, Hiss DC, Bardien S, Ekpo OE. Rutin as a Potent Antioxidant: Implications for Neurodegenerative Disorders. *Oxid Med Cell Longev* 2018; 2018:6241017.
25. Pan PH, Lin SY, Wang YY, Chen WY, Chuang YH, Wu CC, et al. Protective effects of rutin on liver injury induced by biliary obstruction in rats. *Free Radic Biol Med* 2014; 73:106-16.
26. Scholten D, Trebicka J, Liedtke C, Weiskirchen R. The carbon tetrachloride model in mice. *Lab Anim* 2015; 49:4-11.
27. Weber LW, Boll M, Stampfl A. Hepatotoxicity and mechanism of action of haloalkanes: carbon tetrachloride as a toxicological model. *Crit Rev Toxicol* 2003; 33:105-36.
28. Basu S. Carbon tetrachloride-induced lipid peroxidation: eicosanoid formation and their regulation by antioxidant nutrients. *Toxicology* 2003; 189:113-27.
29. Novo E, Povero D, Busletta C, Paternostro C, di Bonzo LV, Cannito S, et al. The biphasic nature of hypoxia-induced directional migration of activated human hepatic stellate cells. *J Pathol* 2012; 226:588-97.
30. Lei XG, Zhu JH, Cheng WH, Bao Y, Ho YS, Reddi AR, et al. Paradoxical Roles of Antioxidant Enzymes: Basic Mechanisms and Health Implications. Physiol Rev 2016; 96:307-64.
31. Suzuki T, Motohashi H, Yamamoto M. Toward clinical application of the Keap1-Nrf2 pathway. *Trends Pharmacol Sci* 2013; 34:340-6.
32. Rangasamy T, Cho CY, Thimmulappa RK, Zhen L, Srisuma SS, Kensler TW, et al. Genetic ablation of Nrf2 enhances susceptibility to cigarette smoke-induced emphysema in mice. *J Clin Invest* 2004; 114:1248-59.
33. Ke B, Shen XD, Zhang Y, Ji H, Gao F, Yue S, et al. KEAP1-NRF2 complex in ischemia-induced hepatocellular damage of mouse liver transplants. J Hepatol 2013; 59:1200-7.
34. Shin SM, Yang JH, Ki SH. Role of the Nrf2-ARE pathway in liver diseases. *Oxid Med Cell Longev* 2013; 2013:763257.
35. Alam J, Stewart D, Touchard C, Boinapally S, Choi AM, Cook JL. Nrf2, a Cap'n'Collar transcription factor, regulates induction of the heme oxygenase-1 gene. *J Biol Chem* 1999; 274:26071-8.
36. Mihm S. Danger-Associated Molecular Patterns (DAMPs): Molecular Triggers for Sterile Inflammation in the Liver. *Int J Mol Sci* 2018; 19.
37. Morio LA, Chiu H, Sprowles KA, Zhou P, Heck DE, Gordon MK, et al. Distinct roles of tumor necrosis factor-alpha and nitric oxide in acute liver injury induced by carbon tetrachloride in mice. *Toxicol Appl Pharmacol* 2001; 172:44-51.
38. Wree A, McGeough MD, Inzaugarat ME, Eguchi A, Schuster S, Johnson CD, et al. NLRP3 inflammasome driven liver injury and fibrosis: Roles of IL-17 and TNF in mice. *Hepatology* 2018; 67:736-749.
39. Mridha AR, Wree A, Robertson AAB, Yeh MM, Johnson CD, Van Rooyen DM, et al. NLRP3 inflammasome blockade reduces liver inflammation and fibrosis in experimental NASH in mice. *Journal of hepatology* 2017; 66:1037-1046.

40. Wree A, Eguchi A, McGeough MD, Pena CA, Johnson CD, Canbay A, et al. NLRP3 inflammasome activation results in hepatocyte pyroptosis, liver inflammation, and fibrosis in mice. *Hepatology* 2014; 59:898-910.
41. Gaul S, Leszczynska A, Alegre F, Kaufmann B, Johnson CD, Adams LA, et al. Hepatocyte pyroptosis and release of inflammasome particles induce stellate cell activation and liver fibrosis. *Journal of hepatology* 2021; 74:156-167.
42. Huang Y, Xu W, Zhou R. NLRP3 inflammasome activation and cell death. *Cell Mol Immunol* 2021; 18:2114-2127.
43. Miao EA, Rajan JV, Aderem A. Caspase-1-induced pyroptotic cell death. *Immunol Rev* 2011; 243:206-14.
44. Bala S, Csak T, Saha B, Zatsiorsky J, Kodys K, Catalano D, et al. The pro-inflammatory effects of miR-155 promote liver fibrosis and alcohol-induced steatohepatitis. *J Hepatol* 2016; 64:1378-87.
45. Mills EL, Ryan DG, Prag HA, Dikovskaya D, Menon D, Zaslona Z, et al. Itaconate is an anti-inflammatory metabolite that activates Nrf2 via alkylation of KEAP1. *Nature* 2018; 556:113-117.
46. Liao ST, Han C, Xu DQ, Fu XW, Wang JS, Kong LY. 4-Octyl itaconate inhibits aerobic glycolysis by targeting GAPDH to exert anti-inflammatory effects. *Nat Commun* 2019; 10:5091.
47. Qin W, Zhang Y, Tang H, Liu D, Chen Y, Liu Y, et al. Chemoproteomic Profiling of Itaconation by Bioorthogonal Probes in Inflammatory Macrophages. *J Am Chem Soc* 2020; 142:10894-10898.
48. Qin W, Qin K, Zhang Y, Jia W, Chen Y, Cheng B, et al. S-glycosylation-based cysteine profiling reveals regulation of glycolysis by itaconate. *Nat Chem Biol* 2019; 15:983-991.
49. Yang W, Wang Y, Zhang P, Sun X, Chen X, Yu J, et al. Immune-responsive gene 1 protects against liver injury caused by concanavalin A via the activation Nrf2/HO-1 pathway and inhibition of ROS activation pathways. *Free Radic Biol Med* 2022; 182:108-118.
50. Hooftman A, Angiari S, Hester S, Corcoran SE, Runtsch MC, Ling C, et al. The Immunomodulatory Metabolite Itaconate Modifies NLRP3 and Inhibits Inflammasome Activation. *Cell Metab* 2020; 32:468-478.e7.

Tables

Table 1. The primer sequences used for real-time PCR

Gene	Forward Primers (5’–3’)	Reverse Primers (5’–3’)
GAPDH	AGG TCG GTG TGA ACG GAT TTG	TGT AGA CCA TGT AGT TGA GGT CA
IL-1β	GCA ACT GTT CCT GAA CTC AAC T	ATC TTT TGG GGT CCG TCA ACT
IL-6	TAG TCC TTC CTA CCC CAA TTT CC	TTG GTC CTT AGC CAC TCC TTC
TNF-α	CCC TCA CAC TCA GAT CAT CTT CT	GCT ACG ACG TGG GCT ACA G
CCL2	TTA AAA ACC TGG ATC GGA ACC AA	GCA TTA GCT TCA GAT TTA CGG GT
Col1a1	GCT CCT CTT AGG GGC CAC T	CCA CGT CTC ACC ATT GGG G
CTGF	TCT CCA CCC GAG TTA CCA ATG	AAT GTT TTC CTC CAG GTC AGC
TGF-b	TTG CTT CAG CTC CAC AGA GA	TGG TTG TAG AGG GCA AGG AC
TIMP-1	TGG TTG TAG AGG GCA AGG AC	TGG TTG TAG AGG GCA AGG AC

Figures

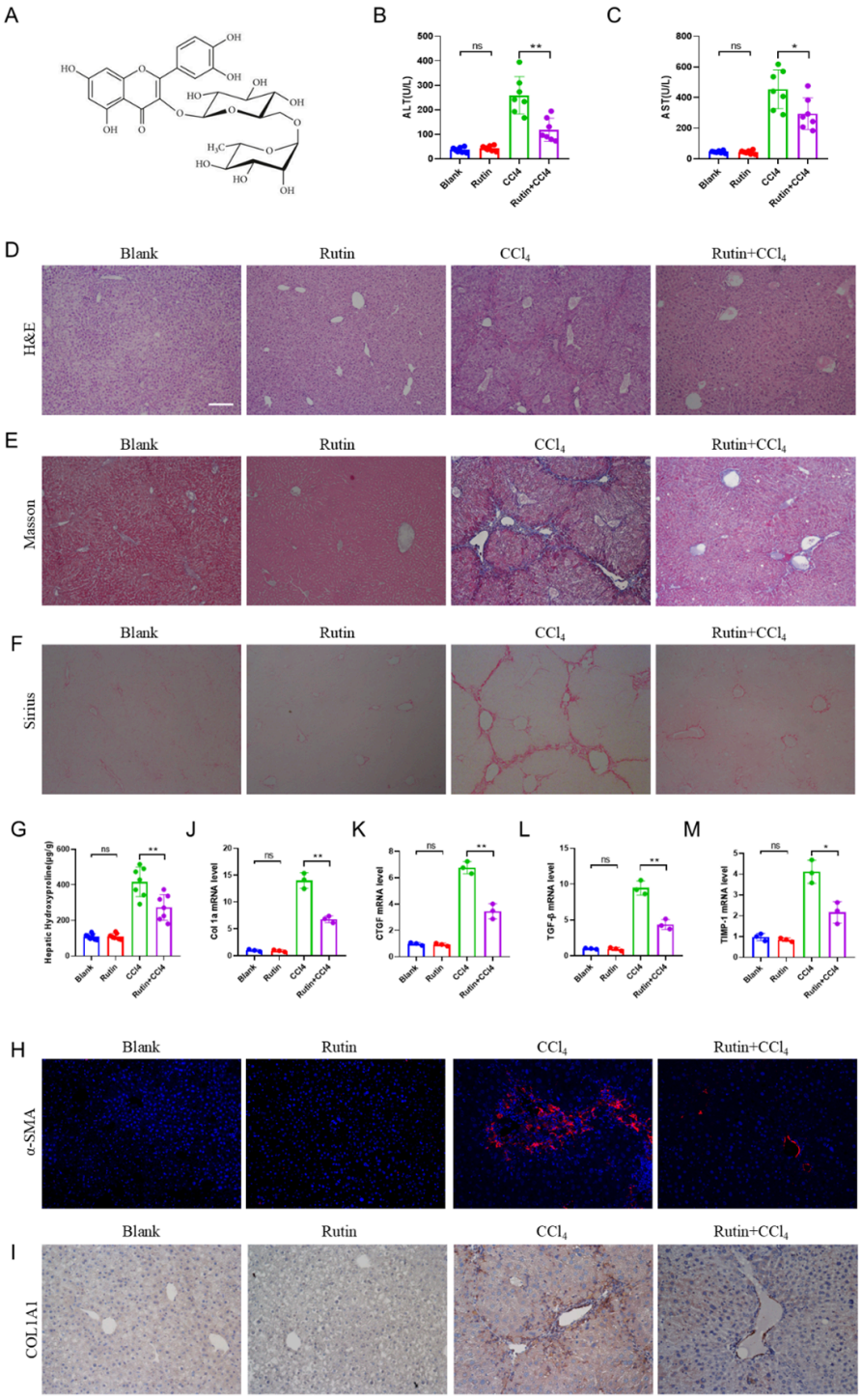


Figure 1

Rutin attenuates CCl_4-induced liver injury and fibrosis in mice.

(A) Chemical structure of Rutin. (B) Serum ALT levels. (C) Serum AST levels. (D) H&E staining. (E) Masson staining. (F) Sirius Red staining. (G) Hepatic hydroxyproline content. (H) α-SMA (IHC). (I–M)

mRNA levels of Col1a1, CTGF, TGF-β, and TIMP-1 (RT-qPCR). Data were expressed as mean ± SD; n = 6. *$P < 0.05$.

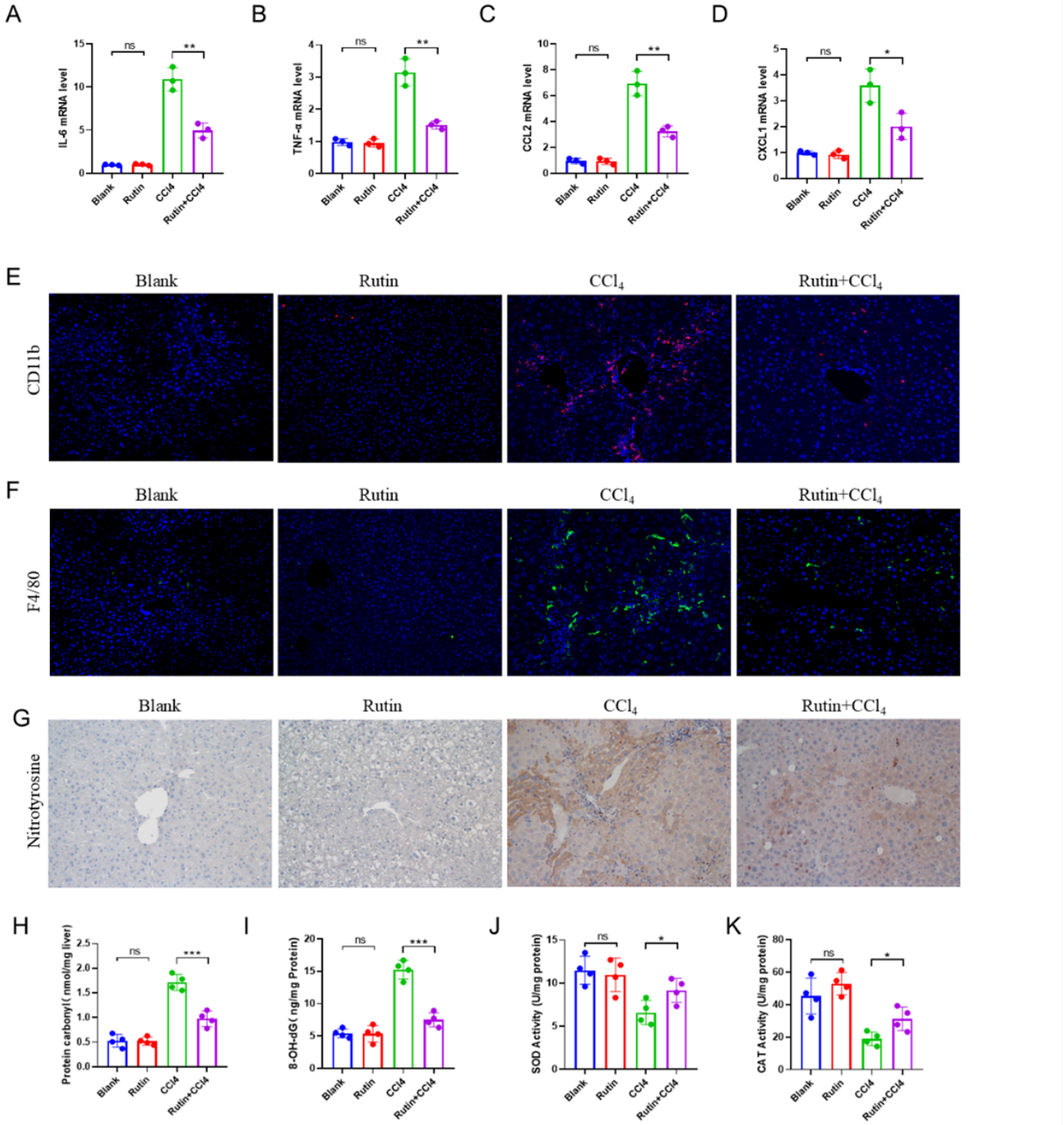


Figure 2

Rutin reduces hepatic inflammation and oxidative stress in CCl_4-treated mice.

(A–D) mRNA levels of IL-6, TNF-α, CCL2, and CXCL1 (RT-qPCR). E. Hepatic neutrophils (IHF). F. Hepatic macrophages (IHF). (G) 4-HNE expression (IHC). (H) Protein carbonyl levels (ELISA). (I) Hepatic levels of the nucleic acid oxidation product 8-OH-dG (ELISA). (J) SOD activity. (K) CAT activity. Data were expressed as mean ± SD; n = 6. *$P < 0.05$.

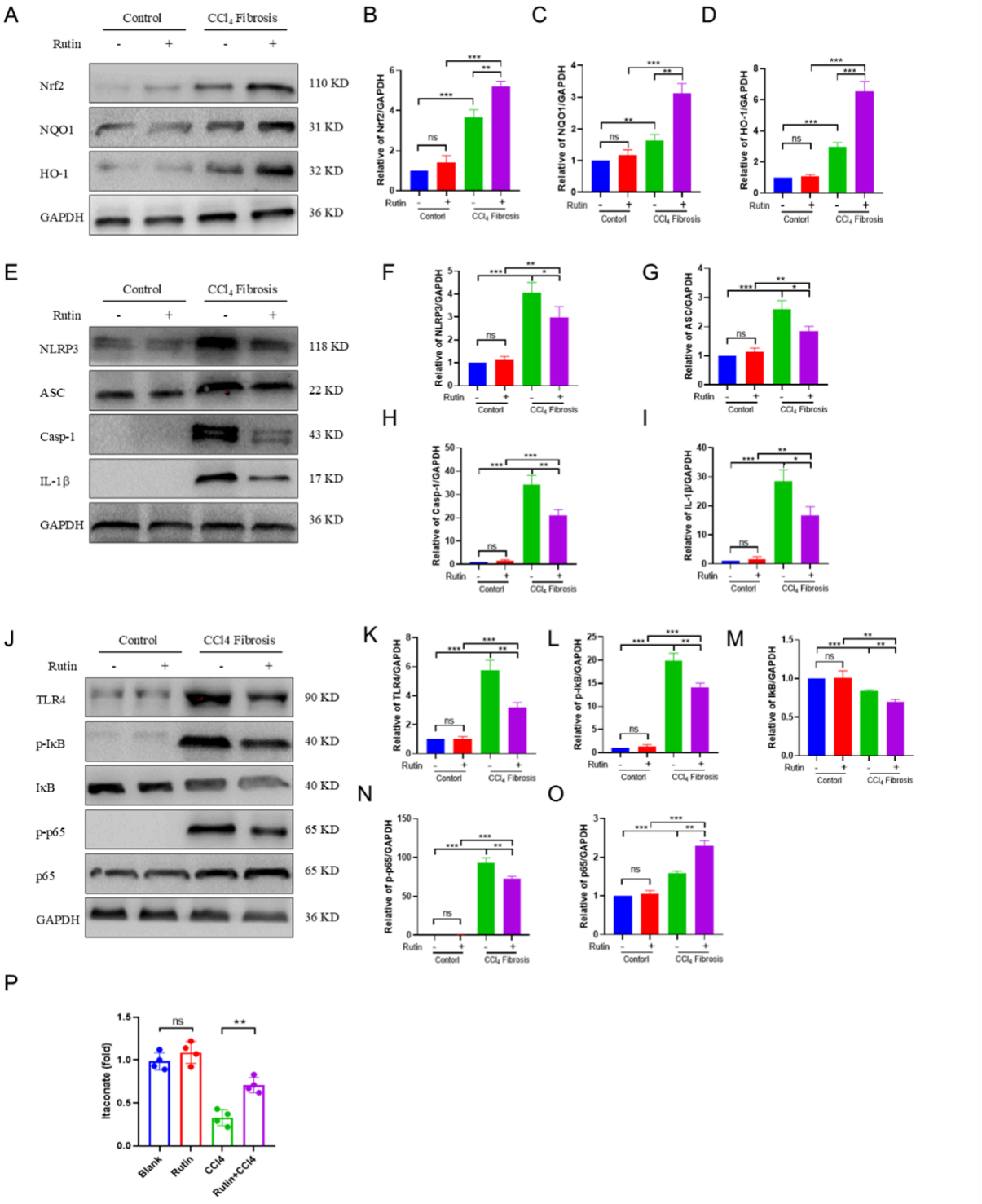
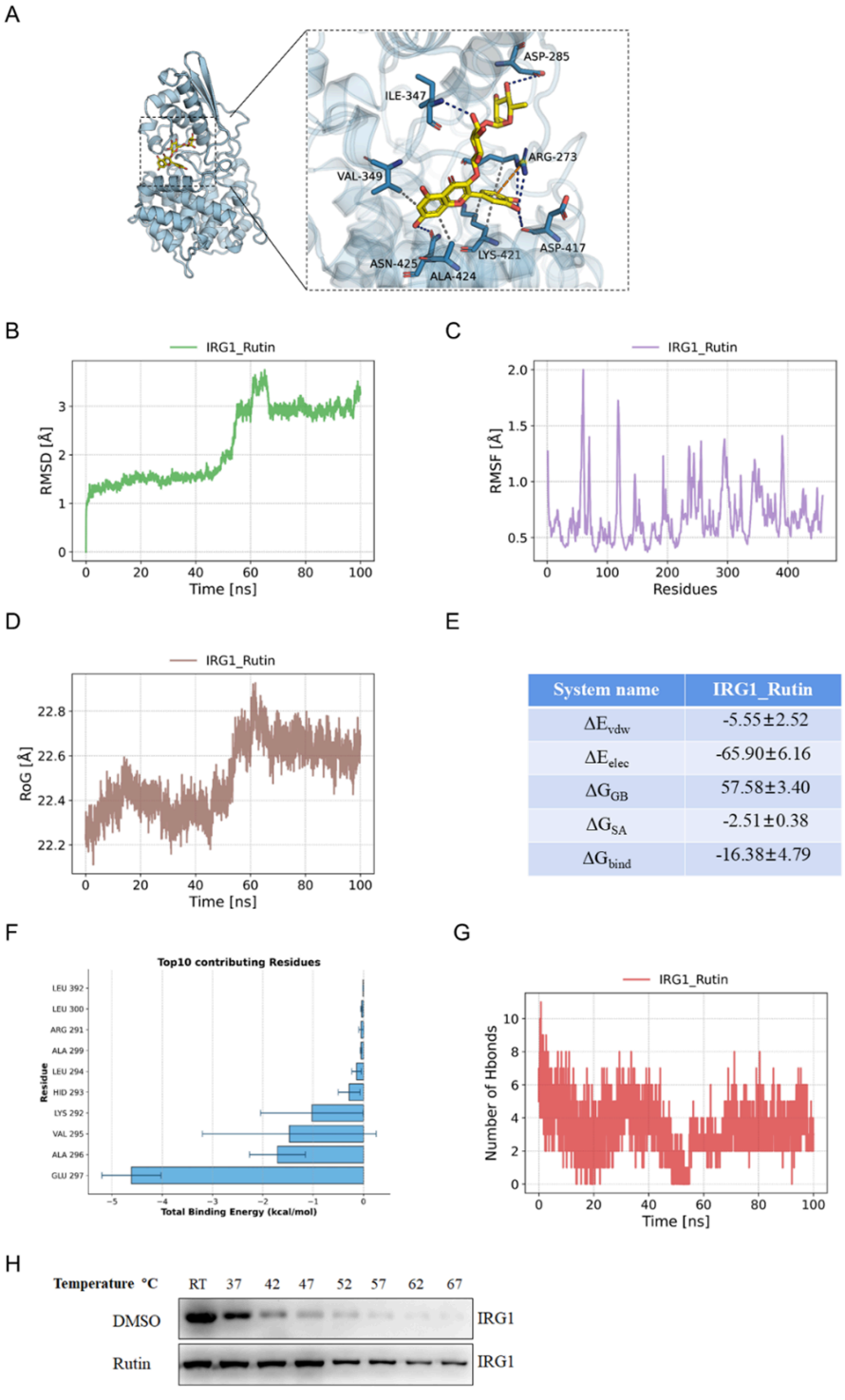


Figure 3

Rutin activates Nrf2 and inhibits the NLRP3-NF-κB pathway in CCl_4-treated mice.

(A) Nrf2, NQO1, and HO-1 protein levels (WB). (B–D) Quantification of Nrf2, NQO1, and HO-1. (E) NLRP3, ASC, and pro-caspase-1 protein levels (WB). (F–I) Quantification of NLRP3, ASC, caspase-1, and IL-1β. (J) TLR4, IκB, and p65 protein levels (WB). (K–M) Quantification of TLR4, IκB, and p65. (N) Hepatic itaconate levels (HPLC). Data were expressed as mean ± SD; n = 3. *P < 0.05.



System name	IRG1_Rutin
ΔE_{vdw}	-5.55±2.52
ΔE_{elec}	-65.90±6.16
ΔG_{GB}	57.58±3.40
ΔG_{SA}	-2.51±0.38
ΔG_{bind}	-16.38±4.79

Figure 4

Molecular interaction between Rutin and IRG1.

(A) Molecular docking analysis. (B) RMSD of the Rutin-IRG1 complex. (C) RMSF of IRG1 residues. (D) Radius of gyration (RoG). (E) Binding energy (MM-GBSA). (F) Key residues contributing to binding. (G) Hydrogen bond dynamics. (H) CETSA showing IRG1 thermal stability.

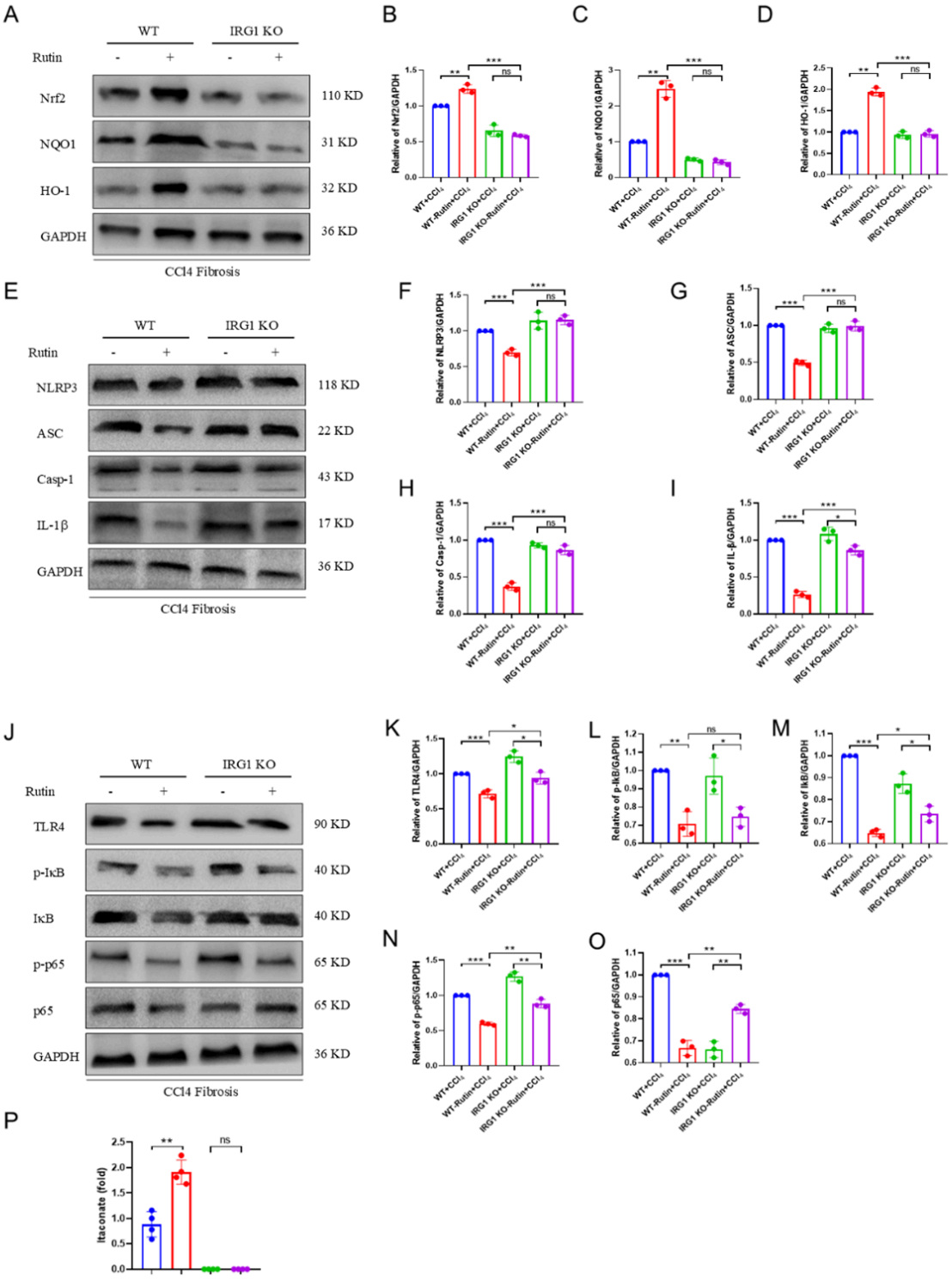


Figure 5

IRG1 is required for Rutin-mediated activation of Nrf2 and inhibition of the NLRP3–NF-κB pathway.

(A) Nrf2, NQO1, and HO-1 protein levels (WB). (B–D) Quantification of Nrf2, NQO1, and HO-1. (E) NLRP3, ASC, and pro-caspase-1 protein levels (WB). (F–I) Quantification of NLRP3, ASC, pro-caspase-1, and IL-1β. (J) TLR4, IκB, and p65 protein levels (WB). (K–M) Quantification of TLR4, IκB, and p65. (N) Hepatic itaconate levels (HPLC). Data were expressed as mean ± SD; n = 3. *$P < 0.05$.

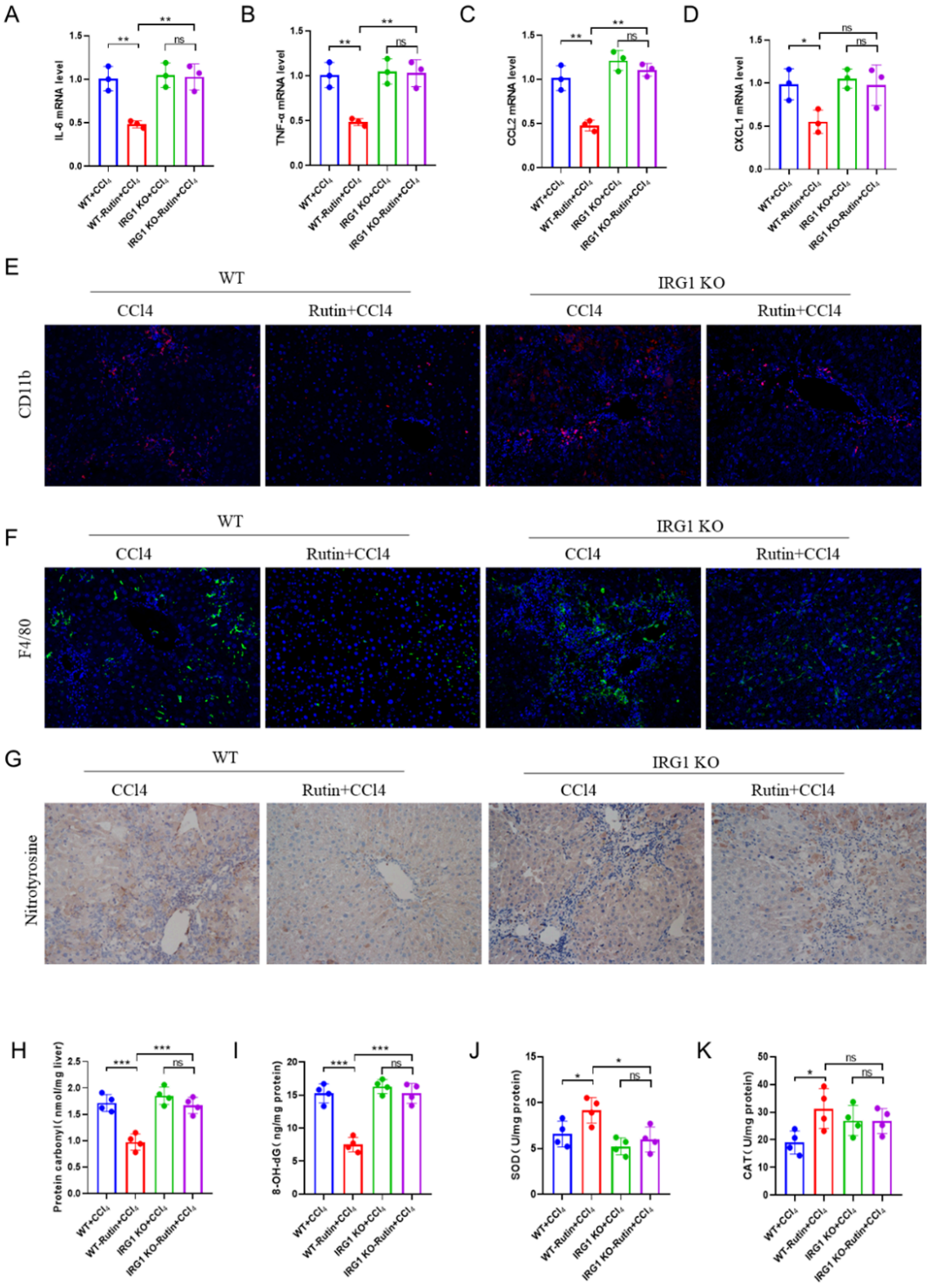


Figure 6

IRG1 is required for the anti-inflammatory and antioxidant effects of Rutin.

(A, B) Hepatic mRNA levels of IL-6 and TNF-α (RT-qPCR). (C, D) Hepatic mRNA levels of CCL2 and CXCL1 (RT-qPCR). (E) Hepatic neutrophils (IHF). (F) Hepatic macrophages (IHF). (G) Hepatic 4-HNE levels (IHC). (H) Hepatic protein carbonyl levels (ELISA). (I) Hepatic 8-OH-dG levels (ELISA). (J) Hepatic SOD activity.

(K) Hepatic CAT activity. Data were expressed as mean ± SD; n = 6. *P < 0.05.

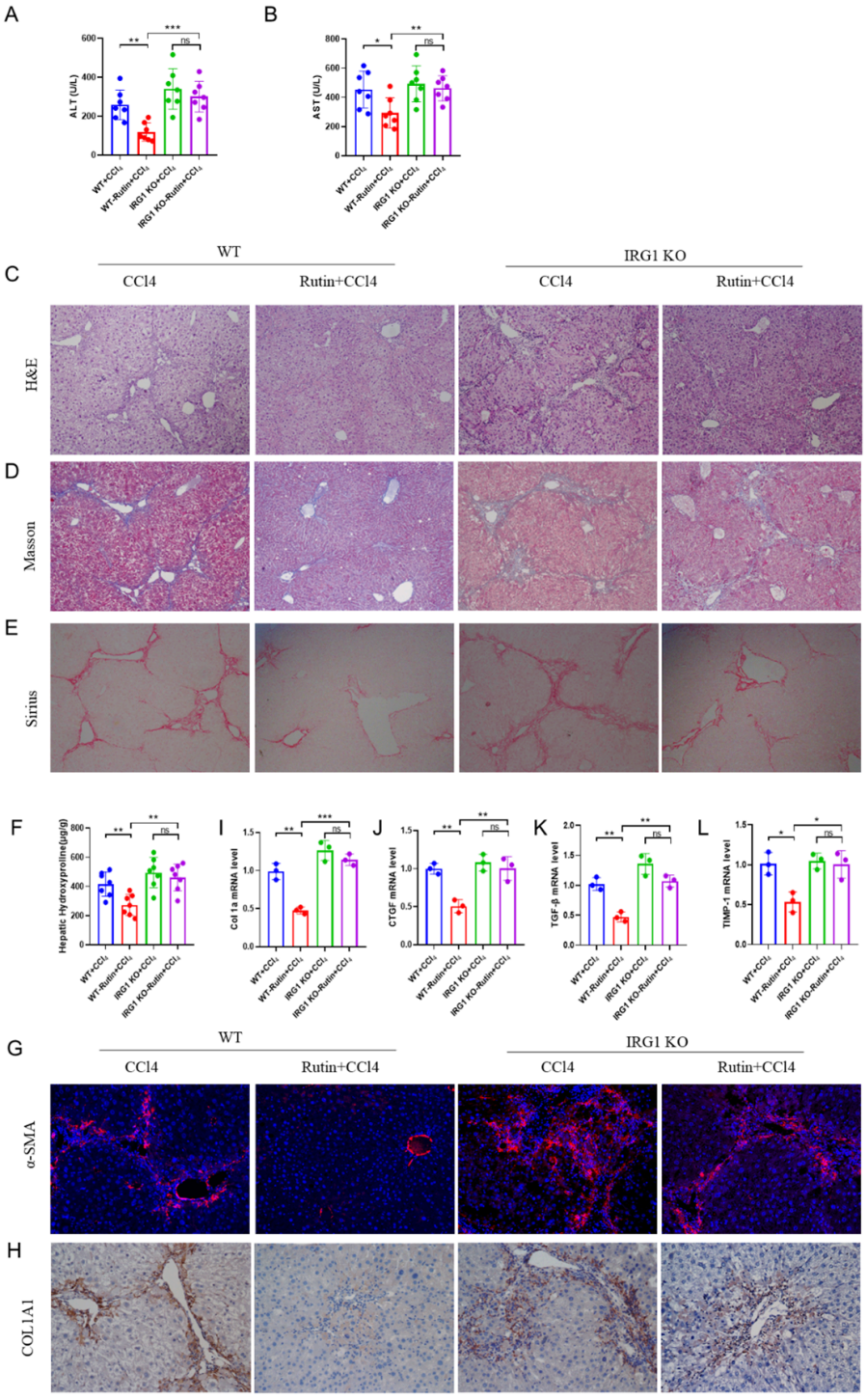


Figure 7

IRG1 deficiency impairs the hepatoprotective and antifibrotic effects of Rutin.

(A) Serum ALT levels. (B) Serum AST levels. (C) H&E staining of liver tissue. (D) Masson staining. (E) Sirius Red staining. (F) Hepatic hydroxyproline content. (G) α-SMA expression (IHC). (H–K) mRNA levels of Col1a1, CTGF, TGF-β, and TIMP-1 (RT-qPCR). (L) Mechanistic summary diagram. Data were expressed as mean ± SD; n = 6. *$P < 0.05$.

Supplementary Files

This is a list of supplementary files associated with this preprint. Click to download.

- GA.docx